CJC Chinese Journal of Chemistry 中国化学 - An International Journal

For submission: https://mc.manuscriptcentral.com/cjoc
For published articles: https://onlinelibrary.wiley.com/journal/16147065

Concise Report

Cite this paper: *Chin. J. Chem.* **2021**, *39*, 1273—1280. **DOI: 10.1002/cjoc.202000643**

Bridging from the Sequence to Architecture: Graft Copolymers Engineering *via* Successive Latent Monomer and Grafting-from Strategies†

Yajie Zhang,[a] Xiaohuan Cao,[a] Yang Gao,[a] Yujie Xie,[a] Zhihao Huang,*[,a] Zhengbiao Zhang,*[,a,b] and Xiulin Zhu[a,c]

[a] *State and Local Joint Engineering Laboratory for Novel Functional Polymeric Materials, Jiangsu Key Laboratory of Advanced Functional Polymer Design and Application, College of Chemistry, Chemical Engineering and Materials Science, Soochow University, Suzhou, Jiangsu 215123, China*
[b] *State Key Laboratory of Radiation Medicine and Protection, Soochow University, Suzhou, Jiangsu 215123, China*
[c] *Global Institute of Software Technology, No. 5 Qingshan Road, Suzhou National Hi-Tech District, Suzhou, Jiangsu 215163, China*

Keywords

Sequence determination | Polymers | Latent Monomer | Polymerization | Maleimide

Main observation and conclusion

The on-demand building copolymer structures, from sequence to architecture, is crucial in understanding the relation between polymer structure and property, meanwhile motivating the innovation of polymer hierarchy. However, the challenge is conspicuous for complicated polymer structures from inherently intricate polymerization. In this work, copolymers with tailored grafting density and distributions were achieved using successive latent monomer and grafting-from strategies. The hydroxyl group functionalized furan/maleimide adduct (FMOH) was selected as the latent monomer for RAFT polymerization of an array of copolymers with tailored localization of hydroxyl group along the main chain. The hydroxyl group further initiated the ring opening polymerization (ROP) of *L*-lactide or *ε*-caprolactone, resulting in a library of multicomponent copolymers *via* grafting-from strategy. The initiating efficiency reached to ~100% with variable molecular weight (21 300—58 600 Da) and narrow distributions ($Đ_M$ < 1.25), indicating that such graft copolymers possessed controlled density and distribution of side chains as its linear template. The investigation on thermal properties of the well-defined graft copolymers implied that the precise tailoring over copolymer structures at the molecule level could lead to tunable chemical/physical properties. This work bridged polymer from sequence to architecture, unveiled a new method in creating graft copolymers with programmable structures and provided the insight into the structure/property relationship.

Comprehensive Graphic Content

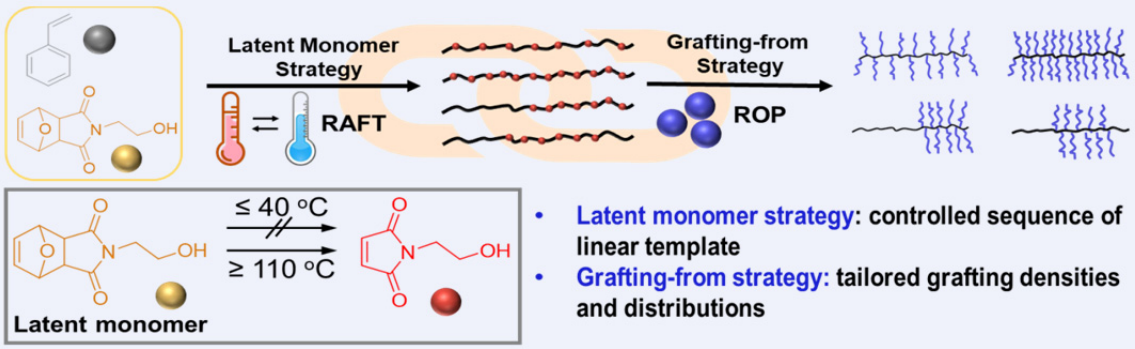

*E-mail: zhhuang@suda.edu.cn; zhangzhengbiao@suda.edu.cn
† Dedicated to the special issue of Polymer Synthesis.

View HTML Article | Supporting Information

Background and Originality Content

Precise control over polymer sequence and architecture is essential for both understanding the structure-property relationship and designing optimal materials.[1-3] Graft copolymers, constructed by grafted polymeric side chains on the linear backbone, are one of the important polymer topologies which benefited from exquisite control over the structures, therefore exhibiting diverse and variable self-assembled morphologies, solution behaviors as well as mechanical properties.[4-5] They have become an area of great interests especially in supersoft elastomers,[6] rheology control agents,[7-8] biosensors,[9-10] lubricants[11] and drug-delivery materials.[12-14] Meanwhile, regulation of the density and distribution is decisive to the performance of graft copolymers, including mechanical properties, physical behaviors, self-assembly process and stimuli-responsive properties.[5,15-21]

Various strategies and chemistries have been developed toward the graft copolymers with controlled density and distribution.[22-28] For instance, Perrier and co-workers have prepared a library of poly(styrene-*co*-maleic anhydride) by RAFT polymerization with controlled sequence and architectures including alternating, diblock, multiblock, multisite, and alternating star. These polymers were subsequently functionalized with long aliphatic alcohols *via* grafting-onto strategy, leading to well-defined architectures with controlled side group density and distribution.[26] Taking advantage of the different reactivity of co-monomer pairs, Grubbs and co-workers demonstrated an efficient grafting-through approach for simultaneously controlling the grafting density and side chain distribution by ring opening metathesis polymerization of norbornene-functionalized macro-monomer and norbonernenyl diester.[29-30] Kamigaito and co-workers reported the synthesis of ABB periodically graft copolymers by direct radical copolymerization of functionalized limonene (A) and maleimide derivatives (B) in fluorinated alcohol and subsequently allowed for a grafting-from installation of poly(methyl methacrylate) side chain.[31] Based on grafting-onto strategy for sequence regulation *via* living anionic polymerization, three architectures with similar number of SiH functional groups per chain but totally different sequence, *i.e.*, gradient, tandem and symmetrical structures, were successfully achieved by Ma and coworkers.[32]

Essentially, the control over the density and distribution of side chains is the programmable placement of co-monomer units along the main chain, namely sequence control. Despite the formidable task as next "Holy Grail" or one of the "ultimate goals" in polymer synthesis, the sequence control over the polymer structures has received intense attention in recent years, largely on account of their enticing properties.[1,33-39] Tremendous efforts have been devoted and many methodologies have been developed for sequence-controlled polymers, including controlled monomer addition,[40-41] template monomers[42-47] and hydrogen bonding regulation.[31,36-37,48-53] In 2017, our group proposed a latent monomer strategy to achieve the sequence controlled goal.[54-58] The furan/maleimide adduct was regarded as the latent monomer, which was inhibited for radical polymerization at low temperature. After elevating temperature, the polymerizable maleimide can be released *via* the retro Diels-Alder (*r*DA) reaction. The *in-situ* released maleimide was immediately involved in the polymerization, thus creating the desired placements of maleimide motifs along the growing chain. Such latent monomer strategy endowed a building platform for tailored sequence in a non-invasive and one-shot feeding manner.

Herein, we bridged the polymeric architecture with programmable sequence by successive control over the latent monomer as well as grafting-from strategies, leading to the constructions of architectures with tailored side chain density and controlled distribution (Scheme 1). The furan/*N*-(2-hydroxyehtyl) maleimide adduct (FMOH) was selected as the latent monomer for generating an array of sequence-controlled polymers *via* RAFT polymerization of styrene (St) and FMOH with programmable temperature change. In the sequence-controlled polymers, the *N*-(2-hydroxyehtyl) maleimide (MOH) was deposited along the polymer chain with controlled distributions. The hydroxyl groups of MOH further efficiently initiated the ring opening polymerization (ROP) of *L*-lactide (*L*-LA) or *ε*-caprolactone (*ε*-CL) to extend the side chains on the polymer. As a consequence, graft copolymers with controlled side chain density and distribution were synthesized (Scheme 1). This work endowed a general and adaptable platform for building well-defined architectures, advancing the methodology research on precision polymer synthesis.

Scheme 1 Schematic illustration on the construction of well-defined polymeric architectures *via* successive control over latent monomer as well as grafting-from strategies

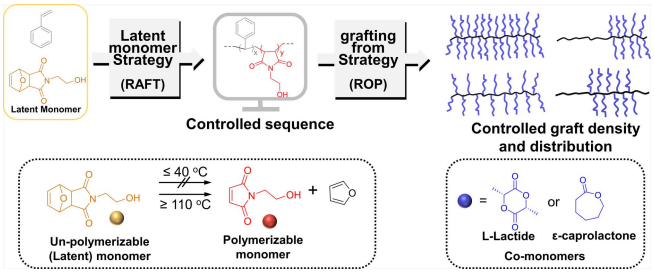

Results and Discussion

In this work, the latent monomer (FMOH) bearing initiating moiety for grafting side chain was synthesized and characterized (Scheme S1 and Figures S1—S2).[57] The temperature-dependent *r*DA reaction for releasing maleimide was identified through the ^{1}H NMR. Approximately 93% of FMOH was converted to maleimide *via r*DA reaction within 10 h at 110 °C, while no remarkable *r*DA reaction was observed at 40 °C within 60 h (Figure S3). This result confirmed the strong temperature dependence of *r*DA reaction, guaranteeing the sequence controlled strategy and the desired placement of MOH along the polymer chain by programmable change of temperature (Figure 1A).

The RAFT polymerization of St and FMOH ($[St]_0/[FMOH]_0$ = 100 : 10) was firstly conducted at 110 °C (Table 1, entry 1). The conversion of St and FMOH was determined by ^{1}H NMR (Figure S4). As conveyed in Figure 1B, the consumption of FMOH synchronized with St conversion at 110 °C, which resulted in the polymer sequence with averagely distributed MOH units. The cumulative (F_{cum}) and instaneous (F_{inst}) contents of FMOH were displayed in Figure 1C, which clearly confirmed the statistical placements of MOH units with 14.2% incorporated into the polymer chain. The good livingness of the RAFT polymerization was proved by size exclusion chromatography (SEC), which confirmed the uniformity of the chain-to-chain sequence structure (Figure S5). The final polymer (**L1**) was purified by precipitation and rigorously characterized by SEC and ^{1}H NMR (Figure 2 and Figure S6). As mentioned, the *r*DA reaction for releasing polymerizable MOH monomer was temperature dependent, which provided the possibility to manipulate the sequence of the structures by programmable polymerization temperature. A temperature sequence of 40 °C (36.5 h)—110 °C (7.0 h) was employed for synthesis of the sequence-controlled diblock polymer, *i.e.*, **L2** (Table 1, entry 2). As depicted in Figure 1D, during the 1st slot (40 °C, 36.5 h), RAFT polymerization of St proceeded slowly and no MOH was released. As a result, a homo-polystyrene block was created in the 1st slot, which was confirmed by the existence of St repeating units in

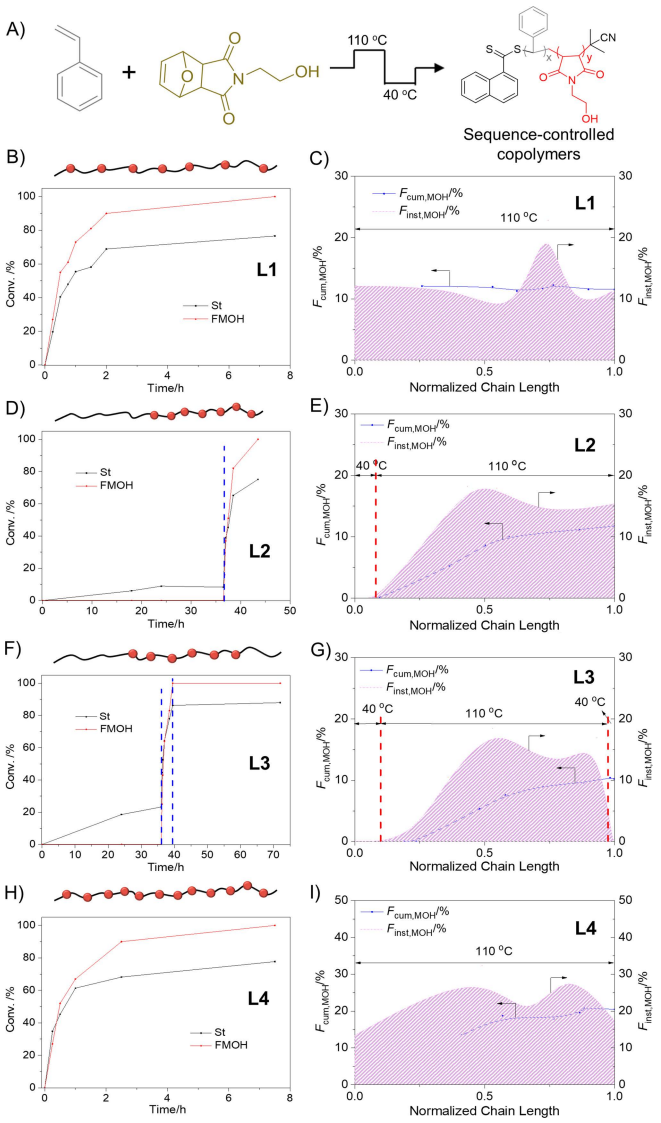

Figure 1 Sequence-controlled polymers through latent monomer strategy (A). Kinetic plots of the copolymers (B, D, F, H) with temperature sequence: 110 °C (B and H); 40 °C—110 °C (D); 40 °C—110 °C—40 °C (F). Cumulative (F_{cum}) and instantaneous (F_{inst}) contents of MOH as a function of normalized chain length) (C, E, G, I). $[St]_0/[FMOH]_0/[CPDN]_0/[ACHN]_0$ = 100/10/1/0.2, St = 5.0 mL, in DMF, DMF/St (1/1, *V*/*V*) (B, D, F) $[St]_0/[FMOH]_0/[CPDN]_0/[ACHN]_0$ = 100/20/1/0.2, St = 5.0 mL, in DMF, DMF/St (1/1, *V*/*V*) (H). The model diagram of polymer chains is not accurate but as the general illustration. The F_{inst} profile has been smoothed.

MALDI-TOF mass spectra (104.09 Da, Figure S7). The reaction was further moved to a pre-stabilized oil bath at 110 °C, for another 7.0 h (2nd slot). Upon transferring to 110 °C, the *r*DA reaction was initiated and MOH was gradually released and immediately polymerized with St. Therefore, the second block containing both St and MOH units was formed. The sequence was also verified by the changes in $F_{inst,\ MOH}$ and $F_{cum,\ MOH}$ with the normalized chain length (Figure 1E). The target polymer contained approximately 14.5% of MOH content. SEC traces in Figure S8 indicated the good livingness of this polymerization. Moreover, the triblock copolymer **L3** was also pre-designed and created with temperature sequence of 40 °C (36.0 h)—110 °C (3.5 h)—40 °C (32.5 h) (Table 1, entry 3 and Figures S10—S11). As shown in Figure 1F, during the 1st slot, a homo PS segment was formed and no releasing of MOH was observed. In the 2nd slot, the polymerization was exposed to 110 °C (3.5 h), and FMOH gradually released MOH, which copolymerized with St to form a hetero-block. The polymerization temperature was changed back to 40 °C (32.5 h) at the final stage. Similar to the 1st slot, the *r*DA reaction for releasing MOH was ceased. Therefore, a second homo-PS segment was fabricated as the third block. This triblock sequence structure was also confirmed by $F_{inst,\ MOH}$ and $F_{cum,\ MOH}$ contents of MOH with normalized chain lengths (Figure 1G). The polymer (**L4**) with similar sequence to **L1** but higher MOH content (23.6%) was successfully synthesized under the identical condition by only increasing the feed ratio from $[St]_0/[FMOH]_0$ = 100 : 10 to 100 : 20 (Figures 1H—1I and S12—S13) (Table 1, entry 4). Meanwhile, another diblock copolymer (**L5**) with the similar MOH distribution but higher MOH content (22.7%) (Table 1, entry 5) was also successfully synthesized by increasing the feed ratio with $[St]_0/[FMOH]_0$ = 100 : 20 (Table 1 and Figures S14—S16). These results established that the latent monomer FMOH could be utilized for sequence regulation, and the content of MOH can be readily manipulated by changing the feed ratio of the co-monomers.

In summary, by intentionally manipulating the temperature of polymerization, five sequence-controlled polymers, *i.e.*, averagely distributed (**L1**, **L4**), diblock (**L2**, **L5**) and triblock (**L3**), with different molecular weights (~10 400—15 400 Da), MOH contents (~14.2%—23.6%) and distributions were created (Table 1). All the sequence-controlled polymers were purified by precipitation and rigorously characterized by SEC and ^{1}H NMR. The SEC elution profile showed narrow and unimodal traces (Figure 2A). Characteristic resonances from the terminal naphtyl group (a, δ 8.02—7.60), hydroxyl groups in MOH units (b, δ 4.85—4.50) and phenyl groups of PS (c, δ 7.43—6.10) were clearly identified (Figure 2B and Figures S6, S9, S11, S13, S15).

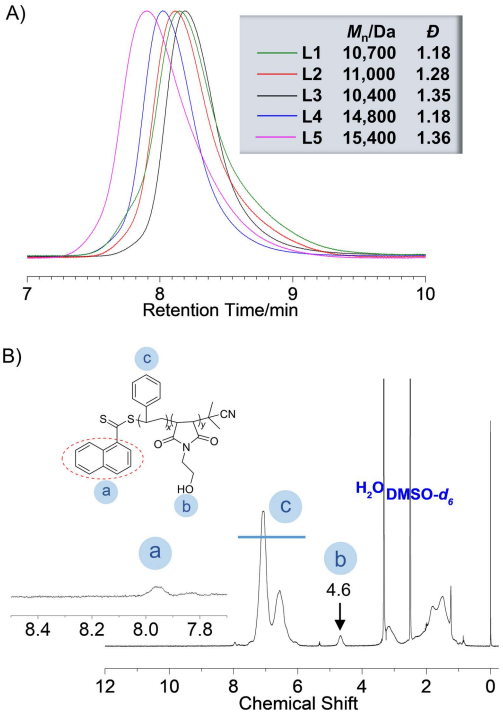

Figure 2 SEC traces of sequence-controlled polymers (A). The ^{1}H NMR spectrum of **L1** in DMSO-d_6 (300 MHz) (B).

Aliphatic polyesters from lactones or lactides have long been attractive in both industry and academia as a consequence of their good biodegradability, biocompatibility as well as unique thermal properties.[59-65] In this work, poly(*L*-LA) (PLLA) or poly(ε-CL) (PCL) was designed as the side chains of the graft copolymer. The hydroxyl groups with controlled locations on the sequence-controlled polymers were used as initiating sites for the

ring opening polymerization (ROP) of *L*-LA or *ε*-CL (Figure 3A). The ROP was performed under the [OH]/[L-LA] molar ratio of 1 : 20 at 40 °C for 48 h. For the ROP of *ε*-CL, the [OH]/[ε-CL] feed molar ratio changed to 1 : 80 and polymerized by using $Sn(Oct)_2$ as the catalyst at 100 °C (Supplemental Information Section A3.3). An array of graft copolymers was readily obtained *via* grafting-from strategy.

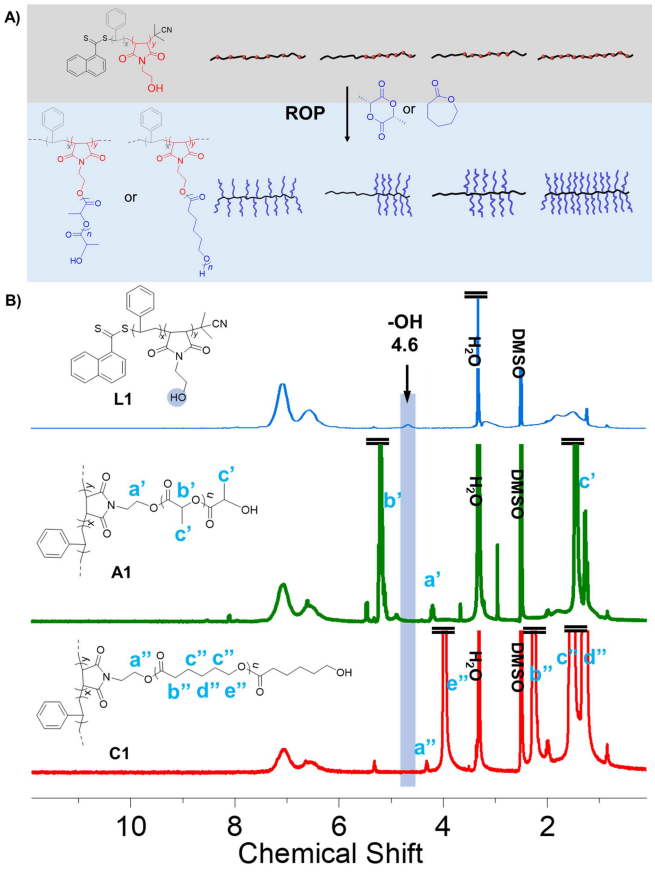

Figure 3 ROP of *L*-LA or *ε*-CL for well-defined architectures *via* grafting-from strategy (A). ^{1}H NMR spectra of **L1**, **A1** and **C1** in DMSO-d_6 (300 MHz) (B).

The structures of the graft copolymers were verified by SEC and ^{1}H NMR (Figures S17—S19), and the results are listed in Table 2. The ^{1}H NMR spectra of typical graft copolymers (**A1** and **C1**) as well as linear precursor (**L1**) are presented in Figure 3B. Compared with the precursor, the resonance signals at *δ* 5.20 (b′), 1.45—1.24 (c′) are ascribed to PLLA in **A1**. Meanwhile, the *δ* 3.96 (e″), 2.25 (b″), 1.50 (c″) and 1.29 (d″) are assigned to the characteristic signals of the methylenes in PCL segments in **C1**. These results confirmed the successful grafting of side chains to the **L1**. More importantly, grafting efficiency reached to almost 100% according to the disappearance of the proton resonance at *δ* 4.60, which was assigned to the hydroxyl group in MOH moieties. These results demonstrated that the graft copolymers possessed controlled density and distribution of side chains, inheriting from the corresponding sequence-controlled linear precursors. The degree of polymerization (DP) and the composition ratio of side chain were calculated from ^{1}H NMR (Figures S17—S18). Moreover, the SEC curves of the graft copolymers derived from **L1** were presented in Figure S19a. Unimodal, symmetrical, and narrow distributed SEC traces (*Đ* < 1.25) as well as an apparent molecular weight shift were obtained. The graft copolymers with similar molecular weights, dispersity and side chain compositions ($f_{PCL/PLLA}$), but with different precursors are listed in Table 2. Meanwhile, the graft copolymer **A4** resulted in the higher MW and content of side chain than its analogue **A1**, owing to the higher MOH content of its linear precursor. Similar graft copolymers with controlled grafting density and distribution were also obtained using PCL as the side chains. These results confirmed that the sequence-controlled polymers could be used as the ideal template for constructing well-defined architectures *via* grafting-from strategy.

Table 1 Summary of the sequence-controlled polymers (SCPs) created by latent monomer strategy

Entry	SCPs	$[St]_0/[FMOH]_0$ [a]	$F_{cum,MOH}$ [b]/%	$M_{n,SEC}$ [c]/Da	*Đ* [c]	T_g [d]/°C
1	**L1**	100 : 10	14.24	10 700	1.18	118.0
2	**L2**	100 : 10	14.48	11 000	1.28	117.8
3	**L3**	100 : 10	13.71	10 400	1.35	111.8
4	**L4**	100 : 20	23.55	14 800	1.18	133.6
5	**L5**	100 : 20	22.68	15 400	1.36	133.8

[a] $[CPDN]_0/[ACHN]_0$ = 1/0.2, St = 5.0 mL, in DMF, DMF/St (1/1, *V*/*V*). [b] Calculated by *in situ* ^{1}H NMR. [c] Determined by SEC with St standard calibration. [d] T_g was characterized by DSC.

An array of graft copolymers with predetermined side chain densities and distributions was demonstrated in this study through the programmable latent monomer and grafting-from strategies, which could be ideal for precisely discovering the relationship regarding the polymer structures and properties. Especially, the study of the thermal properties of polymers with similar MWs and compositions but different topologies necessitated the applications of the different polymer architectures. In this work, the thermal properties of the graft copolymers were evaluated by differential scanning calorimetry (DSC) (Figures S20—S21). As shown in Figure 4A and Table 1, the incorporation of MOH units remarkably increased the glass transition temperature (T_g) to 111.8—133.8 °C, comparing with the T_g of homo-PS (95.7 °C) for the sequence-controlled polymers, as the consequence of the incorporation of the heat–resistant maleimide units.[55] More MOH units resulted in higher T_g, 118.0 °C for **L1** and 133.6 °C for **L4**. For sequence-controlled polymers with similar MOH contents but different monomer distribution, **L3** has a relatively lower T_g at 111.8 °C as it contains two homo-PS segments, which leads to a more flexible chain than the other two linear polymers (**L1** and **L2**).

Table 2 Summary of the graft copolymers created by successive latent monomer and grafting-from strategies

Graft copolymers		$M_{n,SEC}$ [a]/Da	*Đ* [a]	$DP_{LA/CL}$ [b]	$f_{PLLA/PCL}$ [b]/%	$T_{g/m}$ [c]/°C	T_c [c]/°C
Grafted PLLA	**A1**	21 300	1.16	9	42.5	50.8	—
	A2	21 700	1.23	8	38.5	52.2	—
	A3	22 000	1.24	9	39.9	59.2	—
	A4	27 800	1.18	7	52.8	55.4	—
	A5	30 600	1.24	6	47.6	59.1	—
Grafted PCL	**C1**	49 800	1.24	56	86.8	51.7	19.8
	C2	47 100	1.20	56	85.8	51.3	18.2
	C3	49 200	1.15	49	88.5	51.0	17.5
	C4	50 700	1.22	37	87.6	49.0	11.8
	C5	58 600	1.24	37	90.6	48.5	11.3

[a] Determined by SEC with St standard calibration. [b] Determined by ^{1}H NMR. [c] T_g, T_m and T_c (T_g was for sequence-controlled polymers and grafted PLLA copolymers, while T_m and T_c were for grafted PCL copolymers) were characterized by DSC.

For graft copolymers (Figure 4A and Table 2), taking grafted PLLA series as an example, a significant drop in T_g was observed for grafted PLLA copolymers compared with their corresponding

linear precursors due to the homo PLLA side chain (T_g: 50—80 °C).[66-67] Furthermore, **A1** (brush-like), **A2** (tadpole-like) and **A3** (linear-brush-linear) with similar grafting density but different distribution displayed different T_g. **A3** possessing a linear-brush-linear type topology displayed the highest T_g (59.2 °C), while brush-like **A1** had the lowest T_g (50.8 °C) (Table 2 and Figure 4A). It has been reported that entanglements in amorphous polymers could affect the relative chain motion in the glassy state.[68] Here, the two homo-PS segments of **A3** might cause more entanglements than **A2**, which decreased the flexibility of the graft copolymers and reflected a higher T_g value. In grafted PCL system, **C3** with linear-brush-linear type topology demonstrated the lowest T_c than other analogues (**C1** and **C2**). Such decrease could be attributed to the entanglements, which induced crystalline imperfections during the crystallization (f_{PCL} > 80%) (Figure 4B).[22,61,69-70] The results indicated that the thermal properties could be tuned by regulating the grafting density and distribution.

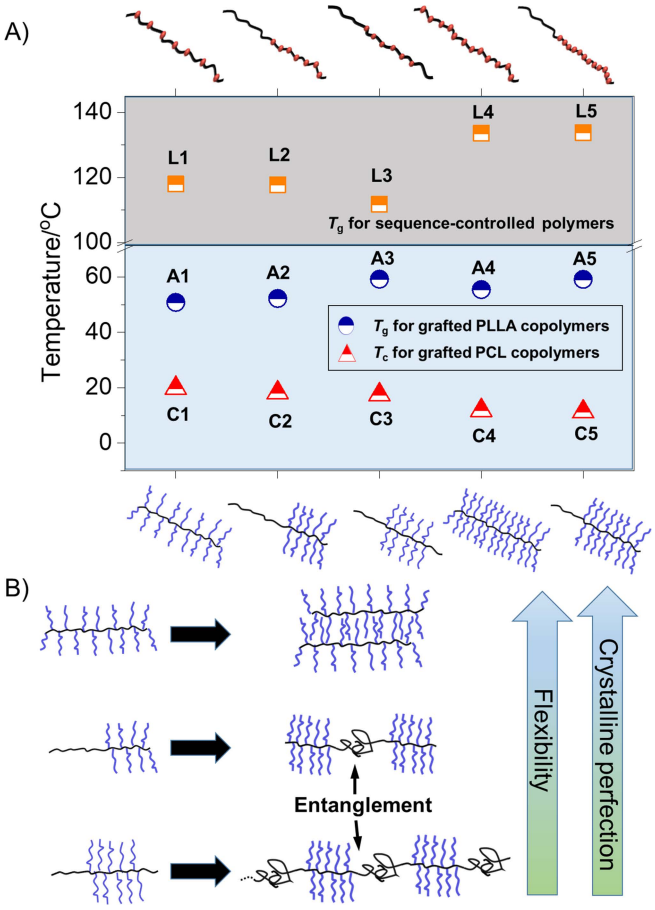

Figure 4 DSC results of graft copolymers and their corresponding sequence-controlled polymers, in the second heating run (A). Proposed explanation of the different thermal behaviors within the different topologies of graft copolymers (B).

Conclusions

In this study, we demonstrated the construction of well-defined polymeric architectures with controlled density and distribution of side chains by successive control over latent monomer as well as grafting-from strategies. The latent monomer allowed to produce a series of linear polymers with predetermined locations of the pendent hydroxyl groups, which could further initiate the ROP of *L*-LA or *ε*-CL for the PLLA or PCL side chains *via* grafting-from strategy. The initiating efficiency of hydroxyl group reached to approximately 100%, guaranteeing the controlled distribution of the side chains from the linear precursor. The on-demand architectures resulted in the different thermal properties such as the crystallization or glass transition, which provided the insight in exploring the structure-property relationship. This work offered a general and adaptable platform for graft polymers engineering with tailored side chain density and distributions, endowing an example for building variable polymers architecture with well-defined properties.

Experimental

General procedure for the synthesis of FM

Furan (64.0 g, 0.94 mol) was added to a solution of maleic anhydride (40.0 g, 0.41 mol) in diethyl ether (300 mL), and the mixture was stirred at room temperature for 41 h. After the reaction was completed, the solid was filtered through the suction filtration and washed with dry ether (3×20 mL). Compound **FM** was dried and obtained as a white solid (57.20 g, 84.4% yield). ^{1}H NMR (300 MHz, $CDCl_3$) δ: 6.58 (t, 2H), 5.46 (t, 2H), 3.18 (s, 2H).

General procedure for the synthesis of FMOH

Compound **FM** (30.0 g) was added to 300 mL of anhydrous methanol. The suspension was cooled to 0 °C. A mixed solution of ethanolamine and anhydrous methanol (volume ratio of 1 : 1) was slowly added dropwise to the suspension. The reaction mixture was then returned to room temperature and stirred for 0.5 h. The reaction solution was further refluxed at 70 °C for 14 h. After the completion of the reaction, the resulted solution was cooled to room temperature and placed in an ice bath for crystallization. The solid was filtered through suction filtration, washed with cold methanol and dried. The resulting white solid was the monomer **FMOH** (25.80 g, 68.3% yield). ^{1}H NMR (300 MHz, DMSO-d_6) δ: 6.55 (s, 2H), 5.12 (s, 2H), 4.77 (t, 1H), 3.50—3.36 (d, 4H), 2.92 (s, 2H).

Typical procedures for RAFT polymerization of St and FMOH with programmable fluctuations of temperature

The polymerization was carried out in an oven-dried Schlenk tube under argon protection. A general procedure for a St/FMOH di-blocky copolymer was provided. All polymerizations were performed in the glass tube with FMOH (0.914 g, 4.37 mmol), CPDN (0.118 g, 0.437 mmol), St (5.0 mL, 43.7 mmol), ABVN (0.022 g, 0.087 mmol), and DMF (5.0 mL). The mixture was then degassed by three freeze-pump-thaw cycles. The reaction tube was placed in a water bath kept at 40 °C. After a predetermined time, the tube was moved to another pre-stabilized oil bath at 110 °C. To prevent the polymer chain from loss of livingness during the temperature change, we normally add a certain amount of initiator azobis(cyclohexanecarbonitrile) (ACHN). At predetermined intervals, an aliquot was taken out with a syringe under argon, and the reaction was terminated by cooling to −20 °C. The monomer conversion was determined by ^{1}H NMR spectroscopy. The crude copolymer was diluted with THF and precipitated in cold anhydrous MeOH to obtain the pure product, which was further analyzed by SEC and ^{1}H NMR spectroscopy.

Synthesis of graft copolymers

Method for grafting PLLA. The sequence-controlled polymer, *L*-LA and DMAP were added into DCM with the ratio 1 : 20 : 4 (sequence-controlled polymer : *L*-LA : DMAP). The polymerization was carried out in a Schlenk flask at 40 °C for 48 h under argon and terminated after several minutes by removal of heat and exposure to oxygen. The polymer was then precipitated in cold MeOH and dried under vacuum.

Method for grafting PCL. The sequence-controlled polymer,

ε-CL and $Sn(Oct)_2$ were added into toluene with the ratio 1 : 80 : 4 (sequence-controlled polymer : ε-CL : $Sn(Oct)_2$). The polymerization was carried out in a Schlenk flask at 100 °C for 4 h under argon and terminated after several minutes by removal of heat and exposure to oxygen. The polymer was then precipitated in cold MeOH and dried under vacuum.

Supporting Information

The supporting information for this article is available on the WWW under https://doi.org/10.1002/cjoc.202000643.

Acknowledgement

This work was supported by the National Natural Science Foundation of China (21925107 and 21674072), the Collaborative Innovation Center of Suzhou Nano Science and Technology, the China Post-doctoral Science Foundation (2020M671571), the Priority Academic Program Development of Jiangsu Higher Education Institutions (PAPD) and the Program of Innovative Research Team of Soochow University.

References

[1] Lutz, J. F.; Ouchi, M.; Liu, D. R.; Sawamoto, M. Sequence-controlled polymers. *Science* **2013**, *341*, 1238149.

[2] Lutz, J. F.; Lehn, J. M.; Meijer, E. W.; Matyjaszewski, K. From precision polymers to complex materials and systems. *Nat. Rev. Mater.* **2016**, *1*, 16024.

[3] Feng, C.; Huang, X. Y. Polymer Brushes: Efficient Synthesis and Applications. *Acc. Chem. Res.* **2018**, *51*, 2314–2323.

[4] Huang, Y. J.; Mai, Y. Y.; Yang, X. W.; Beser, U.; Liu, J. Z.; Zhang, F.; Yan, D. Y.; Mullen, K.; Feng, X. L. Temperature-Dependent Multidimensional Self-Assembly of Polyphenylene-Based "Rod-Coil" Graft Polymers. *J. Am. Chem. Soc.* **2015**, *137*, 11602–11605.

[5] Daniel, W. F. M.; Burdynska, J.; Vatankhah-Varnoosfaderani, M.; Matyjaszewski, K.; Paturej, J.; Rubinstein, M.; Dobrynin, A. V.; Sheiko, S. S. Solvent-free, supersoft and superelastic bottlebrush melts and networks. *Nat. Mater.* **2016**, *15*, 183–189.

[6] Pakula, T.; Zhang, Y.; Matyjaszewski, K.; Lee, H.; Boerner, H.; Qin, S.; Berry, G. C. Molecular brushes as super-soft elastomers. *Polymer* **2006**, *47*, 7198–7206.

[7] Kobayashi, M.; Terayama, Y.; Hosaka, N.; Kaido, M.; Suzuki, A.; Yamada, N. L.; Torikai, N.; Ishihara, K.; Takahara, A. Friction behavior of high-density poly(2-methacryloyloxyethyl phosphorylcholine) brush in aqueous media. *Soft Matter* **2007**, *3*, 740–746.

[8] Yuan, J.; Xu, Y.; Walther, A.; Bolisetty, S.; Schumacher, M.; Schmalz, H.; Ballauff, M.; Muller, A. H. E. Water-soluble organo-silica hybrid nanowires. *Nat. Mater.* **2008**, *7*, 718–722.

[9] Huang, K.; Rzayev, J. Well-Defined Organic Nanotubes from Multicomponent Bottlebrush Copolymers. *J. Am. Chem. Soc.* **2009**, *131*, 6880–6885.

[10] Liu, M.; Wen, Y. T.; Song, X.; Zhu, J. L.; Li, J. A smart thermoresponsive adsorption system for efficient copper ion removal based on alginate-g-poly(N-isopropylacrylamide) graft copolymer. *Carbohydr. Polym.* **2019**, *219*, 280–289.

[11] Watson, S.; Nie, M. Y.; Wang, L.; Stokes, K. Challenges and developments of self-assembled monolayers and polymer brushes as a green lubrication solution for tribological applications. *RSC Adv.* **2015**, *5*, 89698–89730.

[12] Johnson, J. A.; Lu, Y. Y.; Burts, A. O.; Xia, Y.; Durrell, A. C.; Tirrell, D. A.; Grubbs, R. H. Drug-Loaded, Bivalent-Bottle-Brush Polymers by Graft-through ROMP. *Macromolecules* **2010**, *43*, 10326–10335.

[13] Heinrich, C. D.; Thelakkat, M. Poly-(3-hexylthiophene) bottlebrush copolymers with tailored side-chain lengths and high charge carrier mobilities. *J. Mater. Chem. C* **2016**, *4*, 5370–5378.

[14] Que, Y. R.; Liu, Y. J.; Tan, W.; Feng, C.; Shi, P.; Li, Y. J.; Huang, X. Y. Enhancing Photodynamic Therapy Efficacy by Using Fluorinated Nanoplatform. *ACS Macro Lett.* **2016**, *5*, 168–173.

[15] Noel, A.; Borguet, Y. P.; Wooley, K. L. Self-Reporting Degradable Fluorescent Grafted Copolymer Micelles Derived from Biorenewable Resources. *ACS Macro Lett.* **2015**, *4*, 645–650.

[16] Zhang, Q.; Ran, Q. P.; Zhao, H. X.; Shu, X.; Yang, Y.; Zhou, H. X.; Liu, J. P. pH-induced conformational changes of comb-like polycarboxylate investigated by experiment and simulation. *Colloid Polym. Sci.* **2016**, *294*, 1705–1715.

[17] Paturej, J.; Sheiko, S. S.; Panyukov, S.; Rubinstein, M. Molecular structure of bottlebrush polymers in melts. *Sci. Adv.* **2016**, *2,* e1601478.

[18] Kikuchi, M.; Nakano, R.; Jinbo, Y.; Saito, Y.; Ohno, S.; Togashi, D.; Enomoto, K.; Narumi, A.; Haba, O.; Kawaguchi, S. Graft Density Dependence of Main Chain Stiffness in Molecular Rod Brushes. *Macromolecules* **2015**, *48*, 5878–5886.

[19] Li, Y. J.; Jian, Z. K.; Lang, M. D.; Zhang, C. M.; Huang, X. Y. Covalently Functionalized Graphene by Radical Polymers for Graphene-Based High-Performance Cathode Materials. *ACS Appl. Mater. Interfaces* **2016**, *8*, 17352–17359.

[20] Xu, B. B.; Liu, Y. J.; Sun, X. W.; Hu, J. H.; Shi, P.; Huang, X. Y. Semifluorinated Synergistic Nonfouling/Fouling-Release Surface. *ACS Appl. Mater. Interfaces* **2017**, *9*, 16517–16523.

[21] Tao, D. L.; Feng, C.; Cui, Y. A.; Yang, X.; Manners, I.; Winnik, M. A.; Huang, X. Y. Monodisperse Fiber-like Micelles of Controlled Length and Composition with an Oligo(p-phenylenevinylene) Core via "Living" Crystallization-Driven Self-Assembly. *J. Am. Chem. Soc.* **2017**, *139*, 7136–7139.

[22] Zhang, W.; Li, Y.; Liu, L.; Sun, Q.; Shuai, X.; Zhu, W.; Chen, Y. Amphiphilic Toothbrushlike Copolymers Based on Poly(ethylene glycol) and Poly(ε-caprolactone) as Drug Carriers with Enhanced Properties. *Biomacromolecules* **2010**, *11*, 1331–1338.

[23] Ding, N.; Shentu, B.; Pan, P.; Shan, G.; Bao, Y.; Weng, Z. Synthesis and Crystallization of Poly(vinyl acetate)-g-Poly(L-lactide) Graft Copolymer with Controllable Graft Density. *Ind. Eng. Chem. Res.* **2013**, *52*, 12897−12905.

[24] Liu, N.; Liu, B.; Yao, C.; Cui, D. Immortal Ring-Opening Polymerization of rac-Lactide Using Polymeric Alcohol as Initiator to Prepare Graft Copolymer. *Polymers* **2016**, *8,* 17.

[25] Moriceau, G.; Gody, G.; Hartlieb, M.; Kim, H.; Mastrangelo, A.; Smithb, T.; Perrier, S. Functional multisite copolymer by one-pot sequential RAFT copolymerization of styrene and maleic anhydride. *Polym. Chem.* **2017**, *8*, 4152–4161.

[26] Moriceau, G.; Tanaka, J.; Lester, D.; Pappas, G. S.; Cook, A. B.; O'Hora, P.; Winn, J.; Smith, T.; Perrier, S. Influence of Grafting Density and Distribution on Material Properties Using Well-Defined Alkyl Functional Poly(Styrene-co-Maleic Anhydride) Architectures Synthesized by RAFT. *Macromolecules* **2019**, *52*, 1469−1478.

[27] Ogura, Y.; Terashima, T.; Sawamoto, M. Amphiphilic PEG-Functionalized Gradient Copolymers *via* Tandem Catalysis of Living Radical Polymerization and Transesterification. *Macromolecules* **2017**, *50*, 822–831.

[28] Xu, B. B.; Feng, C.; Huang, X. Y. A versatile platform for precise synthesis of asymmetric molecular brush in one shot. *Nat. Commun.* **2017**, *8*, 333.

[29] Chang, A. B.; Lin, T. P.; Thompson, N. B.; Luo, S. X.; Liberman-Martin, A. L.; Chen, H. Y.; Lee, B.; Grubbs, R. H. Design, Synthesis, and Self-Assembly of Polymers with Tailored Graft Distributions. *J. Am. Chem. Soc.* **2017**, *139*, 17683–17693.

[30] Lin, T. P.; Chang, A. B.; Chen, H. Y.; Liberman-Martin, A. L.; Bates, C. M.; Voegtle, M. J.; Bauer, C. A.; Grubbs, R. H. Control of Grafting Density and Distribution in Graft Polymers by Living Ring-Opening Metathesis Copolymerization. *J. Am. Chem. Soc.* **2017**, *139*, 3896–3903.

[31] Matsuda, M.; Satoh, K.; Kamigaito, M. Periodically Functionalized and Grafted Copolymers *via* 1:2-Sequence-Regulated Radical Co-

polymerization of Naturally Occurring Functional Limonene and Maleimide Derivatives. *Macromolecules* **2013**, *46*, 5473–5482.

[32] Huang, W.; Ma, H. W.; Han, L.; Liu, P. B.; Yang, L. C.; Shen, H. Y.; Hao, X. Y.; Li, Y. Synchronous Regulation of Periodicity and Monomer Sequence during Living Anionic Copolymerization of Styrene and Dimethyl-[4-(1-phenylvinyl)phenyl]silane (DPE-SiH). *Macromolecules* **2018**, *51*, 3746–3757.

[33] Pfeifer, S.; Lutz, J. F. A facile procedure for controlling monomer sequence distribution in radical chain polymerizations. *J. Am. Chem. Soc.* **2007**, *129*, 9542–9543.

[34] Kleiner, R. E.; Brudno, Y.; Birnbaum, M. E.; Liu, D. R. DNA-templated polymerization of side-chain-functionalized peptide nucleic acid aldehydes. *J. Am. Chem. Soc.* **2008**, *130*, 4646–4659.

[35] Ida, S.; Terashima, T.; Ouchi, M.; Sawamoto, M. Selective radical addition with a designed heterobifunctional halide: a primary study toward sequence-controlled polymerization upon template effect. *J. Am. Chem. Soc.* **2009**, *131*, 10808–10809.

[36] Satoh, K.; Matsuda, M.; Nagai, K.; Kamigaito, M. AAB-sequence living radical chain copolymerization of naturally occurring limonene with maleimide: an end-to-end sequence-regulated copolymer. *J. Am. Chem. Soc.* **2010**, *132*, 10003–10005.

[37] Satoh, K.; Ozawa, S.; Mizutani, M.; Nagai, K.; Kamigaito, M. Sequence-regulated vinyl copolymers by metal-catalysed step-growth radical polymerization. *Nat. Commun.* **2010**, *1*, 6.

[38] Hibi, Y.; Ouchi, M.; Sawamoto, M. Sequence-regulated radical polymerization with a metal-templated monomer: repetitive ABA sequence by double cyclopolymerization. *Angew. Chem. Int. Ed.* **2011**, *50*, 7434–7437.

[39] Nakatani, K.; Ogura, Y.; Koda, Y.; Terashima, T.; Sawamoto, M. Sequence-regulated copolymers *via* tandem catalysis of living radical polymerization and in situ transesterification. *J. Am. Chem. Soc.* **2012**, *134*, 4373–4383.

[40] Zamfir, M.; Lutz, J. F. Ultra-precise insertion of functional monomers in chain-growth polymerizations. *Nat. Commun.* **2012**, *3,* 1138.

[41] Zamfir, M.; Theato, P.; Lutz, J. F. Controlled folding of polystyrene single chains: design of asymmetric covalent bridges. *Polym. Chem.* **2012**, *3*, 1796–1802.

[42] Ogura, Y.; Terashima, T.; Sawamoto, M. Synchronized Tandem Catalysis of Living Radical Polymerization and Transesterification: Methacrylate Gradient Copolymers with Extremely Broad Glass Transition Temperature. *ACS Macro Lett.* **2013**, *2*, 985–989.

[43] Hibi, Y.; Ouchi, M.; Sawamoto, M. A strategy for sequence control in vinyl polymers *via* iterative controlled radical cyclization. *Nat. Commun.* **2016**, *7*, 11064.

[44] Oh, D. Y.; Ouchi, M.; Nakanishi, T.; Ono, H.; Sawamoto, M. Iterative Radical Addition with a Special Monomer Carrying Bulky and Convertible Pendant: A New Concept toward Controlling the Sequence for Vinyl Polymers. *ACS Macro Lett.* **2016**, *5*, 745–749.

[45] Ouchi, M.; Nakano, M.; Nakanishi, T.; Sawamoto, M. Alternating Sequence Control for Carboxylic Acid and Hydroxy Pendant Groups by Controlled Radical Cyclopolymerization of a Divinyl Monomer Carrying a Cleavable Spacer. *Angew. Chem. Int. Ed.* **2016**, *128*, 14804–14809.

[46] Hattori, G.; Hirai, Y.; Sawamoto, M.; Terashima, T. Self-assembly of PEG/dodecyl-graft amphiphilic copolymers in water: consequences of the monomer sequence and chain flexibility on uniform micelles. *Polym. Chem.* **2017**, *8*, 7248–7259.

[47] Kametani, Y.; Nakano, M.; Yamamoto, T.; Ouchi, M.; Sawamoto, M. Cyclopolymerization of Cleavable Acrylate-Vinyl Ether Divinyl Monomer *via* Nitroxide-Mediated Radical Polymerization: Copolymer beyond Reactivity Ratio. *ACS Macro Lett.* **2017**, *6*, 754–757.

[48] Matsuda, M.; Satoh, K.; Kamigaito, M. 1: 2-sequence-regulated radical copolymerization of naturally occurring terpenes with maleimide derivatives in fluorinated alcohol. *J .Polym. Sci. A Polym. Chem.* **2013**, *51*, 1774–1785.

[49] Soejima, T.; Satoh, K.; Kamigaito, M. Main-Chain and Side-Chain Sequence-Regulated Vinyl Copolymers by Iterative Atom Transfer Radical Additions and 1:1 or 2:1 Alternating Radical Copolymerization. *J. Am. Chem. Soc.* **2016**, *138*, 944–954.

[50] Ojika, M.; Satoh, K.; Kamigaito, M. BAB-random-C Monomer Sequence *via* Radical Terpolymerization of Limonene (A), Maleimide (B), and Methacrylate (C): Terpene Polymers with Randomly Distributed Periodic Sequences. *Angew. Chem. Int. Ed.* **2017**, *129*, 1815–1819.

[51] Satoh, K.; Hashimoto, H.; Kumagai, S.; Aoshima, H.; Uchiyama, M.; Ishibashi, R.; Fujiki, Y.; Kamigaito, M. One-shot controlled/living copolymerization for various comonomer sequence distributions *via* dual radical and cationic active species from RAFT terminals. *Polym. Chem.* **2017**, *8*, 5002–5011.

[52] Hashimoto, H.; Takeshima, H.; Nagai, T.; Uchiyama, M.; Satoh, K.; Kamigaito, M. Valencene as a naturally occurring sesquiterpene monomer for radical copolymerization with maleimide to induce concurrent 1:1 and 1:2 propagation. *Polym. Degrad. Stabil.* **2019**, *161*, 183–190.

[53] Satoh, K.; Ishizuka, K.; Hamada, T.; Handa, M.; Abe, T.; Ozawa, S.; Miyajima, M.; Kamigaito, M. Construction of Sequence-Regulated Vinyl Copolymers *via* Iterative Single Vinyl Monomer Additions and Subsequent Metal-Catalyzed Step-Growth Radical Polymerization. *Macromolecules* **2019**, *52*, 3327–3341.

[54] Ji, Y.; Zhang, L.; Gu, X.; Zhang, W.; Zhou, N.; Zhang, Z.; Zhu, X. Sequence-Controlled Polymers with Furan-Protected Maleimide as a Latent Monomer. *Angew. Chem. Int. Ed.* **2017**, *56*, 2328–2333.

[55] Meng, F.; Zhang, Y.; Ding, K.; Liu, B.; Han, F.; He, Y.; Zhou, N.; Zhang, Z.; Zhu, X. One-shot synthesis of sequence-controlled polymers with versatile succimide motifs for post-modifications. *React. Funct. Polym.* **2019**, *134*, 67–73.

[56] Zhang, L.; Ji, Y.; Gu, X.; Zhang, W.; Zhou, N.; Zhang, Z.; Zhu, X. Synthesis of sequence-controlled polymers with pendent “clickable” or hydrophilic groups *via* latent monomer strategy. *React. Funct. Polym.* **2019**, *138*, 96–103.

[57] Han, F.; Shi, Q.; Zhang, L.; Liu, B.; Zhang, Y.; Gao, Y.; Jia, R.; Zhang, Z.; Zhu, X. Stereoisomeric furan/maleimide adducts as latent monomers for one-shot sequence-controlled polymerization. *Polym. Chem.* **2020**, *11*, 1614–1620.

[58] Zhang, L. Q.; Gao, Y.; Huang, Z. H.; Zhang, W.; Zhou, N. C.; Zhang, Z. B.; Zhu, X. L. Controllably Growing Topologies in One-shot RAFT Polymerization *via* Macro-latent Monomer Strategy. *Chinese J. Polym. Sci.* **2021**, *39*, 60–69.

[59] Zhou, S.; Deng, X.; Yang, H. Biodegradable poly(ε-caprolactone)-poly(ethylene glycol) block copolymers: characterization and their use as drug carriers for a controlled delivery system. *Biomaterials* **2003**, *24*, 3563–3570.

[60] Ghoroghchian, P. P.; Li, G.; Levine, D. H.; Davis, K. P.; Bates, F. S.; Hammer, D. A.; Therien, M. J. Bioresorbable vesicles formed through spontaneous self-assembly of amphiphilic poly(ethylene oxide)-block-polycaprolactone. *Macromolecules* **2006**, *39*, 1673–1675.

[61] Yuan, W.; Yuan, J.; Zhang, F.; Xie, X. Syntheses, Characterization, and in vitro Degradation of Ethyl Cellulose-graft-poly(ε-caprolactone)-block-poly(l-lactide) Copolymers by Sequential Ring-Opening Polymerization. *Biomacromolecules* **2007**, *8*, 1101–1108.

[62] Castillo, R. V.; Muller, A. J.; Raquez, J.; Dubois, P. Crystallization Kinetics and Morphology of Biodegradable Double Crystalline PLLA-b-PCL Diblock Copolymers. *Macromolecules* **2010**, *43*, 4149–4160.

[63] Yang, C.; Wu, H.; Sun, J.; Hsiao, H.; Wang, T. Thermo-induced shape-memory PEG-PCL copolymer as a dual-drug-eluting biodegradable stent. *ACS Appl. Mater. Interfaces* **2013**, *5*, 10985–10994.

[64] Gu, J.; Xiao, P.; Chen, P.; Zhang, L.; Wang, H.; Dai, L.; Song, L.; Huang, Y.; Zhang, J.; Chen, T. Functionalization of Biodegradable PLA Nonwoven Fabric as Superoleophilic and Superhydrophobic Material for Efficient Oil Absorption and Oil/Water Separation. *ACS Appl. Mater. Interfaces* **2017**, *9*, 5968–5973.

[65] Shi, J.; Zhang, L.; Xiao, P.; Huang, Y.; Chen, P.; Wang, X.; Gu, J.; Zhang, J.; Chen, T. Biodegradable PLA Nonwoven Fabric with Controllable Wettability for Efficient Water Purification and Photocatalysis Deg-

radation. *ACS Sustainable Chem. Eng.* **2018**, *6*, 2445–2452.
[66] Lee, S. H.; Kim, S. H.; Han, Y. K.; Kim, Y. H. Synthesis and degradation of end-group-functionalized polylactide. *J. Polym. Sci. A Polym. Chem.* **2001**, *39*, 973–985.
[67] Nakayama, Y.; Matsubara, N.; Cai, Z.; Shiono, T.; Inumaru, K.; Shirahama, H. Effect of end-group modification of poly(lactide)s by cinnamoyl chloride on their thermal stability. *Polym. Degrad. Stabil.* **2017**, *141*, 97–103.
[68] Litvinov, V.; Deblieck, R.; Clair, C.; Van den fonteyne, W.; Lallam, A.; Kleppinger, R.; Ivanov, D. A.; Ries, M. E.; Boerakker, M. Molecular Structure, Phase Composition, Melting Behavior, and Chain Entanglements in the Amorphous Phase of High-Density Polyethylenes. *Macromolecules* **2020**, *53*, 5418–5433.
[69] Villarroya, S.; Zhou, J.; Thurecht, K. J.; Howdle, S. M. Synthesis of Graft Copolymers by the Combination of ATRP and Enzymatic ROP in $scCO_2$. *Macromolecules* **2006**, *39*, 9080–9086.
[70] Zhang, J.; Ren, W.; Sun, X.; Meng, Y.; Du, B.; Zhang, X. Fully Degradable and Well-Defined Brush Copolymers from Combination of Living CO_2/Epoxide Copolymerization, Thiol–Ene Click Reaction and ROP of ε-caprolactone. *Macromolecules* **2011**, *44*, 9882–9886.

Manuscript received: November 23, 2020
Manuscript revised: January 6, 2021
Manuscript accepted: January 8, 2021
Accepted manuscript online: January 11, 2021

